Adiabatic interpretation of a two-level atom diode, a laser device for unidirectional transmission of ground-state atoms

A. Ruschhaupt*
Institut für Mathematische Physik, TU Braunschweig, Mendelssohnstrasse 3, 38106 Braunschweig, Germany

J. G. Muga†
Departamento de Química-Física, Universidad del País Vasco, Apartado. 644, 48080 Bilbao, Spain
(Received 25 May 2005; published 10 January 2006)

We present a generalized two-level scheme for an "atom diode," namely, a laser device that lets a two-level ground-state atom pass in one direction, say from left to right, but not in the opposite direction. The laser field is composed of two lateral state-selective mirror regions and a central pumping region. We demonstrate the robustness of the scheme and propose a physical realization. It is shown that the inclusion of a counterintuitive laser field blocking the excited atoms on the left side of the device is essential for a perfect diode effect. The reason for this, the diodic behavior, and the robustness may be understood with an adiabatic approximation. The conditions to break down the approximation, which imply also the diode failure, are analyzed.

DOI: 10.1103/PhysRevA.73.013608 PACS number(s): 03.75.Be, 42.50.Lc

I. INTRODUCTION

In a previous paper [1] we proposed simple models for an "atom diode," a laser device that lets a neutral atom in its ground state pass in one direction (conventionally from left to right) but not in the opposite direction for a range of incident velocities. A diode is a very basic control element in a circuit, so many applications may be envisioned to trap or cool atoms, or to build logic gates for quantum information processing in atom chips or other setups. Similar ideas have been developed independently by Raizen and co-workers [2,3]. While their work has emphasized cooling and phase-space compression, we looked for the laser interactions leading to the most effective diode. This led us to consider first stimulated Raman adiabatic passage (STIRAP) [4] transitions and three-level atoms, although we also proposed a scheme for two-level atoms. In this paper we continue the investigation of the atom diode by generalizing its two-level version and providing possible physical implementations, a stability analysis, and an interpretation of the results in terms of an adiabatic basis.

We restrict the atomic motion, similarly to [1], to one dimension. This occurs when the atom travels in waveguides formed by optical fields [5], or by electric or magnetic interactions due to charged or current-carrying structures [6]. It can be also a good approximation in free space for atomic packets which are broad in the laser direction, perpendicular to the incident atomic direction [7], and quite generally for microwave or radiofrequency transitions with negligible recoil velocities. Three-dimensional effects should not imply a dramatic disturbance, in any case, as we shall analyze elsewhere.

In Sec. II we present the generalized model for a two-level atom diode. In Sec. III we show its "diodic behavior" and we examine the stability with respect to parameter changes. In the main Sec. IV we will see that the behavior of the diode and of several variants, including in particular the ones discussed in [1,2], can be understood and quantified with the aid of an adiabatic basis (equivalently, partially dressed states) obtained by diagonalizing the effective interaction potential. The paper ends with a summary and an appendix on the adiabaticity criterion.

II. THE MODEL

The basic setting can be seen in Fig. 1(a) and 1(b), and consists in principle of three, partially overlapping laser fields (A simplified two-laser device is also possible as discussed below.): two of them are state-selective mirror lasers blocking the excited ($|2\rangle$) and ground ($|1\rangle$) states on the left and right, respectively, of a central pumping laser on resonance with the atomic transition. They are all assumed to be traveling waves perpendicular to the atomic motion direction. The corresponding effective, time independent, interaction-picture Hamiltonian for the two-level atom may be written, using $|1\rangle \equiv \binom{1}{0}$ and $|2\rangle \equiv \binom{0}{1}$, as

$$\boldsymbol{H} = \frac{\hat{p}_x^2}{2m} + \underbrace{\frac{\hbar}{2}\begin{pmatrix} W_1(x) & \Omega(x) \\ \Omega(x) & W_2(x) \end{pmatrix}}_{\boldsymbol{V}(x)}, \tag{1}$$

where $\Omega(x)$ is the Rabi frequency for the resonant transition and the effective reflecting state-selective potentials are $W_1(x)\hbar/2$ and $W_2(x)\hbar/2$ for states $|1\rangle$ and $|2\rangle$, respectively. As the central laser is on resonance with the transition $1 \leftrightarrow 2$, the detuning (the difference between laser frequency and the transition frequency) is zero and does not enter in Eq. (1). $\hat{p}_x = -i\hbar\partial/\partial x$ is the momentum operator and m is the mass (corresponding to Neon in all numerical examples).

A particular realization of Eq. (1) may actually involve only two detuned lasers, a pumping and a Stokes laser [see

*Email address: a.ruschhaupt@tu-bs.de
†Email address: jg.muga@ehu.es

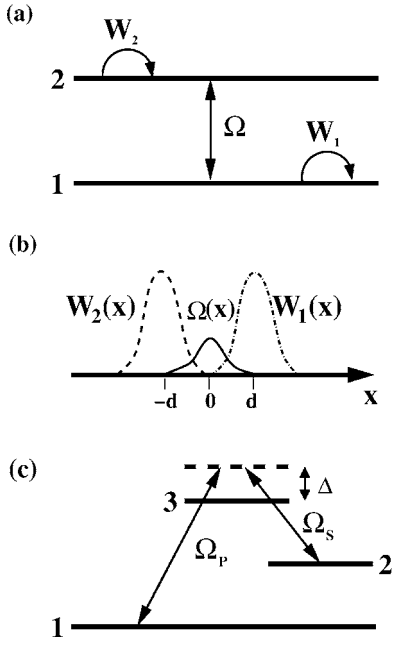

FIG. 1. (a) Schematic action of the different lasers on the atom levels, (b) location of the different laser potentials, and (c) a STIRAP configuration using detuned pumping and Stokes lasers with Rabi frequencies Ω_P and Ω_S.

Fig. 1(c)]. The corresponding stationary Schrödinger equation is given in components by

$$E\Psi_1(x) = \frac{\hat{p}_x^2}{2m}\Psi_1(x) + \frac{\hbar}{2}\Omega_P(x)\Psi_3(x), \tag{2}$$

$$E\Psi_2(x) = \frac{\hat{p}_x^2}{2m}\Psi_2(x) + \frac{\hbar}{2}\Omega_S(x)\Psi_3(x), \tag{3}$$

$$E\Psi_3(x) = \frac{\hat{p}_x^2}{2m}\Psi_3(x) - \hbar\Delta\Psi_3(x) + \frac{\hbar}{2}[\Omega_P(x)\Psi_1(x) + \Omega_S(x)\Psi_2(x)]. \tag{4}$$

In the limit of large detuning $\Delta \gg E/\hbar$, we get from Eq. (4), by following [8],

$$\Psi_3(x) \approx \frac{1}{2\Delta}[\Omega_P(x)\Psi_1(x) + \Omega_S(x)\Psi_2(x)], \tag{5}$$

and, by using Eq. (5) in Eqs. (2) and (3), we can write down an effective, approximate Hamiltonian for the levels 1 and 2. It takes the form of Eq. (1) with $W_1(x) = (1/2\Delta)\Omega_P^2(x)$, $W_2 = (1/2\Delta)\Omega_S^2(x)$, and $\Omega(x) = (1/2\Delta)\Omega_P(x)\Omega_S(x)$. Note that we get the same result by using "adiabatic elimination" [9].

Spontaneous decay is neglected in Eq. (1) for simplicity, but it could be incorporated following [1]. It implies both perturbing and beneficial effects for unidirectional transmission. Notice that in the ideal diode operation the ground-state atom must be excited during its left-to-right crossing of the device. In principle, excited atoms could cross the diode "backwards," i.e., from right to left, but an irreversible decay from the excited state to the ground state would block any backward motion [1].

The behavior of this device is quantified by the scattering transmission and reflection amplitudes for left (l) and right (r) incidence. Using α and β to denote the channels, $\alpha = 1,2$, $\beta = 1,2$, let us denote by $R^l_{\beta\alpha}(v)$ $[R^r_{\beta\alpha}(v)]$ the scattering amplitudes for incidence with modulus of velocity $v > 0$ from the left (right) in channel α, and reflection in channel β. Similarly we denote by $T^l_{\beta\alpha}(v)$ $[T^r_{\beta\alpha}(v)]$ the scattering amplitude for incidence in channel α from the left (right) and transmission in channel β.

For some figures, it will be preferable to use an alternative notation in which the information of the superscript (l/r) is contained instead in the sign of the velocity argument w, positive for left incidence and negative otherwise,

$$R_{\beta\alpha}(w) := \begin{cases} R^l_{\beta\alpha}(|w|) & \text{if } w > 0, \\ R^r_{\beta\alpha}(|w|) & \text{if } w < 0, \end{cases}$$

$$T_{\beta\alpha}(w) := \begin{cases} T^l_{\beta\alpha}(|w|) & \text{if } w > 0, \\ T^r_{\beta\alpha}(|w|) & \text{if } w < 0. \end{cases}$$

The ideal diode configuration must be such that

$$|T^l_{21}(v)|^2 \approx |R^r_{11}(v)|^2 \approx 1, \tag{6}$$

$$|R^l_{\beta 1}(v)|^2 \approx |T^r_{\beta 1}(v)|^2 \approx |R^r_{21}(v)|^2 \approx |T^l_{11}(v)|^2 \approx 0, \tag{7}$$

with $\beta = 1,2$. In words, there must be full transmission for left incidence and full reflection for right incidence in the ground state within an interval $v_{min} < v < v_{max}$ of the modulus of the velocity. More precisely, v_{max}, v_{min} are chosen as the limiting values such that $\Sigma_{\beta=1}^2(|R^l_{\beta 1}|^2 + |T^r_{\beta 1}|^2) + (|R^r_{21}|^2 + |T^l_{11}|^2) + (1 - |T^l_{21}|^2) + (1 - |R^r_{11}|^2) < \epsilon$ for all $v_{min} < v < v_{max}$, where we choose $\epsilon = 0.01$ in the rest of this paper.

III. DIODIC BEHAVIOR AND ITS LIMITS

The behavior of the two-level atom diode is examined by solving numerically the stationary Schrödinger equation,

$$E_v \boldsymbol{\Psi}(x) = \boldsymbol{H}\boldsymbol{\Psi}(x), \tag{8}$$

with the Hamiltonian given by Eq. (1) and $E_v = (m/2)v^2$. We shall use Gaussian laser profiles

$$W_1(x) = \hat{W}_1\Pi(x,d), \quad W_2(x) = \hat{W}_2\Pi(x,-d),$$

$$\Omega(x) = \hat{\Omega}\Pi(x,0),$$

where

$$\Pi(x,x_0) = \exp[-(x-x_0)^2/(2\sigma^2)]$$

and $\sigma = 15$ μm.

The results, obtained by the invariant imbedding method [10,11], are shown in Fig. 2 for different parameters. In the plotted velocity range, the diodic behavior holds, i.e., Eqs. (6) and (7) are fulfilled. (The transmission and reflection

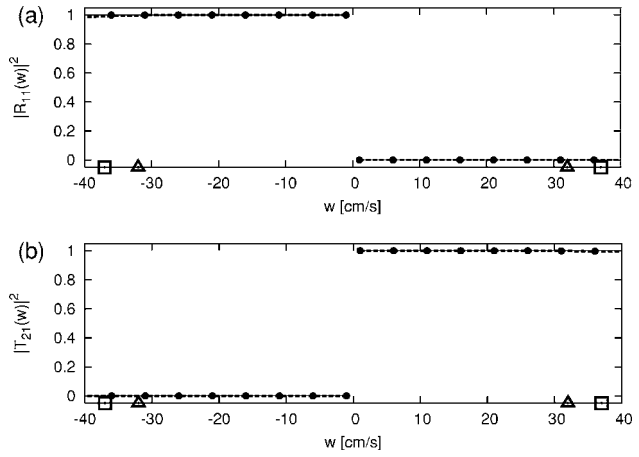

FIG. 2. (a) Reflection probability $|R_{11}(w)|^2$ and (b) transmission probability $|T_{21}(w)|^2$; recall that in this notation $w<0$ corresponds to incidence from the right, and $w>0$ to incidence from the left; $d=50$ μm; $\hat{\Omega}=1\times10^6$/s, $\hat{W}_1=\hat{W}_2=100\times10^6$/s (solid line, $v_{max}=56\pm0.5$ cm/s); $\hat{\Omega}=0.2\times10^6$/s, $\hat{W}_1=20\times10^6$/s, $\hat{W}_2=100\times10^6$/s (dashed line, $\pm v_{max}$, triangles); $\hat{\Omega}=0.2\times10^6$/s, $\hat{W}_1=100\times10^6$/s, $\hat{W}_2=20\times10^6$/s (dots, $\pm v_{max}$, boxes); in all cases $v_{min}<1$ cm/s.

probabilities for incidence in the ground state, $|R_{21}^{l/r}|^2$ and $|T_{11}^{l/r}|^2$, which are not shown in the figure are zero.) The device may be asymmetric, i.e., even with $\hat{W}_1\neq\hat{W}_2$ there can be a diodic behavior (see some examples in Fig. 2).

Note in passing that the device works as a diode for incidence in the excited state too, but in the opposite direction, namely, $|T_{12}^r(v)|^2\approx|R_{22}^l(v)|^2\approx1$, whereas all other probabilities for incidence in the excited state are approximately zero.

Now let us examine the stability of the diode with respect to changes in the separation between laser field centers d. In Fig. 3, v_{max},v_{min} are plotted versus the distance between the laser centers, d, for different combinations of $\hat{\Omega}$, $\hat{W}_1$, and $\hat{W}_2$. For the intensities considered, v_{max} is in the ultracold regime below 1 m/s. In the v_{max} surface, unfilled boxes indicate reflection failure for right incidence and filled circles indicate transmission failure for left incidence. In the v_{min} surface, the failure is always due to transmission failure for left incidence. We see that the valid d range for diodic behavior can be increased by increasing the Rabi frequency $\hat{\Omega}$; compare, e.g., (a) and (b). Moreover, higher mirror intensities increase v_{max} at the plateau but also make it narrower; compare, e.g., (b) and (c). This narrowing can be simply compensated by increasing $\hat{\Omega}$ too; compare, e.g., (a) and (c).

Now, we examine the stability with respect to a shift Δ of the central position of the pumping laser (see Fig. 4). It turns out that there is a range (e.g., $\Delta<12$ μm in Fig. 4) where the limits v_{min} and v_{max} practically do not change.

Finally, we want to examine the stability with respect to a perturbation in the pulse shape. Therefore we choose

$$\Pi(x,x_0)=\exp[-(x-x_0)^2/(2\sigma^2)][1+a(x-x_0)^2/\sigma^2]$$

with $0\leqslant a\leqslant1/2$ such that $0\leqslant\Pi(x,x_0)\leqslant1$. Note that for $a=0$ we get the previously examined Gaussian pulses. The

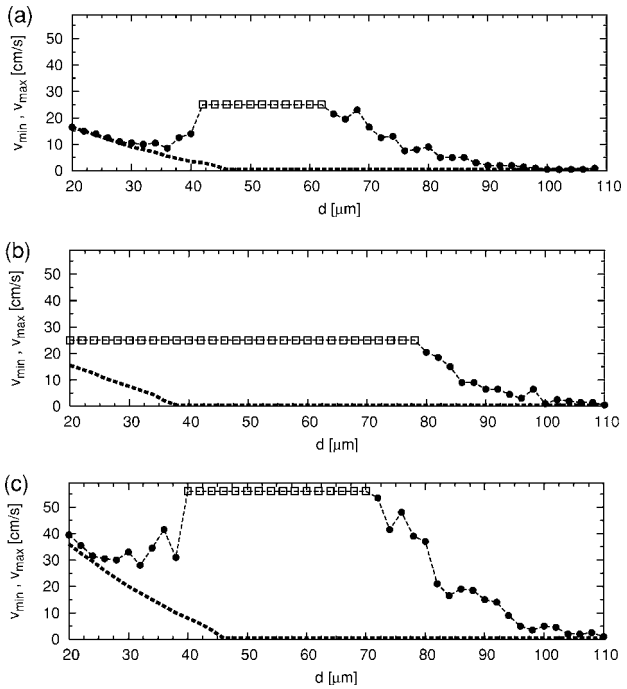

FIG. 3. Limit v_{min} (thick dashed lines) and v_{max} (symbols connected with dashed lines) for diodic behavior; the circles (boxes) correspond to breakdown due to transmission (reflection); (a) $\hat{\Omega}=0.2\times10^6$/s, $\hat{W}_1=\hat{W}_2=20\times10^6$/s; (b) $\hat{\Omega}=1\times10^6$/s, $\hat{W}_1=\hat{W}_2=20\times10^6$/s; (c) $\hat{\Omega}=1\times10^6$/s, $\hat{W}_1=\hat{W}_2=100\times10^6$/s.

corresponding limits v_{min} and v_{max} are shown in Fig. 5. It turns out that $v_{max}\geqslant35$ cm/s for $\alpha\leqslant0.26$. This shows that there is stability concerning changes in the pulse shape. Nevertheless one may optimize the shape to achieve a maximal upper limit. A way to construct these shapes could be the penalty algorithm [12] or by using "local" optimization [13]. Another way to increase the upper limit is by increasing the laser intensities [compare Fig. 3(c) for $d=60$ μm and Fig. 5)] while keeping the Gaussian profile.

IV. ADIABATIC INTERPRETATION OF THE DIODE

A very remarkable and useful property in all cases depicted in Fig. 2 is the constant value of the transmission and reflection probabilities in a broad velocity range. This is call-

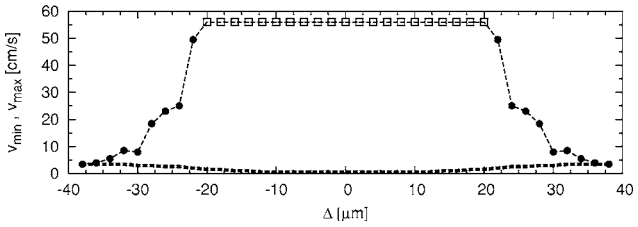

FIG. 4. Limit v_{min} (thick dashed line) and v_{max} (symbols connected with dashed line) for diodic behavior versus the shift Δ for different d; the circles (boxes) correspond to breakdown first for transmission (reflection); $\hat{\Omega}=1\times10^6$/s, $\hat{W}_1=\hat{W}_2=100\times10^6$/s, $d=50$ μm.

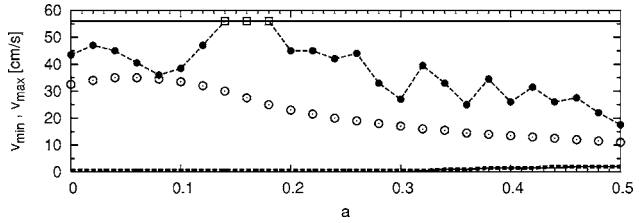

FIG. 5. Limit v_{min} (thick dashed line) and v_{max} (symbols connected with dashed lines) for diodic behavior versus change in the pulse shape a; the filled circles (unfilled boxes) correspond to breakdown first for transmission (reflection); limits of condition (12) $v_{\lambda,min}$ (lower solid line) and $v_{\lambda,max}$ (upper solid line); limit of the adiabatic approximation $v_{ad,max}$ (unfilled circles); $d=60$ μm, $\hat{W}_1=\hat{W}_2=100\times10^6/\mathrm{s}$, $\hat{\Omega}=0.2\times10^6/\mathrm{s}$.

ing for an explanation because, from a classical perspective, the ground-state atom incident from the left—not being affected by W_2—finds first the pumping laser and then the state-selective mirror potential for the ground state. According to this sequential model, one would expect an important effect of the velocity in the pumping efficiency. A different velocity implies a different traversal time and thus a different final phase for the Rabi oscillation, which should lead to a smooth, continuous variation of the final atomic state with the velocity. In particular, the probability of the excited state after the pumping would oscillate with the velocity and therefore the final transmission after the right mirror should oscillate too, if the sequential model picture were valid. The failure of the sequential scattering picture must be due to some sort of quantum interference phenomenon. Interference effects are well known in scattering off composite potentials, but in comparison with, e.g., resonance peaks in a double barrier, the present results are of a different nature.

Moreover there is the question of the role of the mirror potential W_2. If we want ground-state atoms to pass from left to right but not from right to left, it is not intuitively obvious why we should add a reflection potential for the excited state on the left of the pumping potential Ω (see again Fig. 1). To deal with these questions we shall discuss an adiabatic approximation of Eq. (8).

A. Adiabatic approximation

In detail, let us examine the following four cases (labeled depending on the mirror potentials included in the device): case 0: $\hat{W}_1=\hat{W}_2=0$; case 1: $\hat{W}_1>0$, $\hat{W}_2=0$; case 2: $\hat{W}_1=0$, $\hat{W}_2>0$; case 12: $\hat{W}_1>0$, $\hat{W}_2>0$. We diagonalize now the potential matrix $\boldsymbol{V}(x)$

$$\boldsymbol{U}(x)\boldsymbol{V}(x)\boldsymbol{U}^{+}(x)=\begin{pmatrix}\lambda_-(x) & 0\\ 0 & \lambda_+\end{pmatrix}.$$

The orthogonal matrix $\boldsymbol{U}(x)$ is given by

$$\boldsymbol{U}(x)=\begin{pmatrix}\dfrac{W_-(x)-\mu(x)}{\sqrt{4\Omega^2(x)+[W_-(x)-\mu(x)]^2}} & \dfrac{W_-(x)+\mu(x)}{\sqrt{4\Omega^2(x)+[W_-(x)+\mu(x)]^2}}\\ \dfrac{2\Omega(x)}{\sqrt{4\Omega^2(x)+[W_-(x)-\mu(x)]^2}} & \dfrac{2\Omega(x)}{\sqrt{4\Omega^2(x)+[W_-(x)+\mu(x)]^2}}\end{pmatrix}$$

where

$$W_-=W_1-W_2,$$

$$\mu=\sqrt{4\Omega^2(x)+W_-^2(x)},$$

and the eigenvalues of $\boldsymbol{V}(x)$ are

$$\lambda_{\mp}(x)=\frac{\hbar}{4}[W_1(x)+W_2(x)\mp\mu(x)]$$

with corresponding (normalized) eigenvectors $|\lambda_{\mp}(x)\rangle$. The asymptotic form of $\boldsymbol{U}$ varies for the different cases distinguished with a superscript, $U^{(j)}$, $j=0,1,2,12$. For $x\to-\infty$, the same $\boldsymbol{U}$ is found for cases 0 and 1, in which the left edge corresponds to the pumping potential. Similarly, the cases 2 and 12 share the same left edge potential W_2 and thus a common form of $\boldsymbol{U}$,

$$\boldsymbol{U}^{(0,1)}(-\infty)=\frac{1}{\sqrt{2}}\begin{pmatrix}-1 & 1\\ 1 & 1\end{pmatrix},\quad \boldsymbol{U}^{(2,12)}(-\infty)=\begin{pmatrix}-1 & 0\\ 0 & 1\end{pmatrix}.$$

The corresponding analysis for $x\to\infty$ gives the asymptotic forms

$$\boldsymbol{U}^{(0,2)}(\infty)=\frac{1}{\sqrt{2}}\begin{pmatrix}-1 & 1\\ 1 & 1\end{pmatrix},\quad \boldsymbol{U}^{(1,12)}(\infty)=\begin{pmatrix}0 & 1\\ 1 & 0\end{pmatrix}.$$

The eigenvalues $\lambda_{\pm}(x)$ for some parameters are plotted in Fig. 6. We see that $\lambda_+(x)>0$ has at least one high barrier whereas $\lambda_-(x)\approx0$. Note, that if $\Omega(x)=\sqrt{W_1(x)W_2(x)}$ then $\lambda_-(x)=0$ is exactly true.

This recalls the coherent dark states that are used in the three-level STIRAP population transfer [4] where the atom is always in a coherent superposition of two states and never in the remaining third one. In our two-level model there is never a third state. Nevertheless, the advantage of an eigenvector with eigenvalue approximately zero is in both situa-

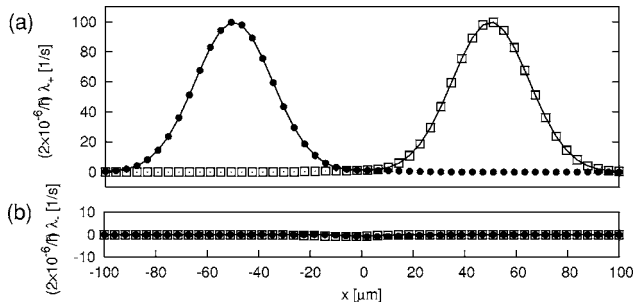

FIG. 6. Eigenvalues (a) λ_+ and (b) λ_-; $d=50\ \mu$m, $\hat{\Omega}=1\times10^6$/s; $\hat{W}_1=\hat{W}_2=100\times10^6$/s (solid lines); $\hat{W}_1=100\times10^6$/s, $\hat{W}_2=0$ (boxes); $\hat{W}_1=0$, $\hat{W}_2=100\times10^6$/s (circles).

tions, the three-level STIRAP transfer and our two-level model, that the atom moves (approximately) freely in that eigenstate avoiding reflection.

If $\boldsymbol{\Psi}$ is a two-component solution of the stationary Schrödinger equation, Eq. (8), we now define the vector

$$\boldsymbol{\Phi}(x)=\begin{pmatrix}\phi_-(x)\\ \phi_+(x)\end{pmatrix}:=\boldsymbol{U}(x)\boldsymbol{\Psi}(x)$$

in a potential-adapted, adiabatic representation. Note that if no approximation is made, $\boldsymbol{\Phi}$ and $\boldsymbol{\Psi}$ are both exact and contain the same information expressed in different bases. Starting from Eq. (8), using $\boldsymbol{\Psi}=\boldsymbol{U}^+\boldsymbol{\Phi}$, and multiplying from the left by $\boldsymbol{U}$, we arrive at the following equation for $\boldsymbol{\Phi}(x)$:

$$E_v\boldsymbol{\Phi}(x)=-\frac{\hbar^2}{2m}\frac{\partial^2}{\partial x^2}\boldsymbol{\Phi}(x)+\begin{pmatrix}\lambda_-(x) & 0\\ 0 & \lambda_+(x)\end{pmatrix}\boldsymbol{\Phi}(x)+\boldsymbol{Q}\boldsymbol{\Phi}(x),$$

where

$$\boldsymbol{Q}=-\frac{\hbar^2}{2m}\left(\boldsymbol{U}(x)\frac{\partial^2\boldsymbol{U}^+}{\partial x^2}(x)+2\boldsymbol{U}(x)\frac{\partial\boldsymbol{U}^+}{\partial x}(x)\frac{\partial}{\partial x}\right)=\begin{pmatrix}mB^2(x)/2 & -A(x)+iB(x)\hat{p}_x\\ A(x)-iB(x)\hat{p}_x & mB^2(x)/2\end{pmatrix}\tag{9}$$

is the coupling term in the adiabatic basis, and $A(x)$, $B(x)$ are real functions,

$$A(x)=\frac{\hbar^2}{2m\mu^4}\left\{2\frac{d\Omega}{dx}\frac{dW_-}{dx}\mu^2+\left(W_-\frac{d^2\Omega}{dx^2}-\Omega\frac{d^2W_-}{dx^2}\right)\times(4\Omega^2+W_-^2)-2\Omega W_-\left[4\left(\frac{d\Omega}{dx}\right)^2-\left(\frac{dW_-}{dx}\right)^2\right]\right\},\tag{10}$$

$$B(x)=\frac{\hbar}{m\mu^2}\left(\Omega\frac{dW_-}{dx}-\frac{d\Omega}{dx}W_-\right).\tag{11}$$

Let us consider incidence from the left and assume first that the coupling $\boldsymbol{Q}$ can be neglected so that there are two independent adiabatic modes ($\pm$) in which the internal state of the atom adapts to the position-dependent eigenstates $|\lambda_\pm\rangle$ of the laser potential $\boldsymbol{V}$, whereas the atom center-of-mass motion is affected in each mode by the effective adiabatic potentials $\lambda_\pm(x)$.

Because $\lambda_-\approx0$, an approximate solution for $\phi_-(x)$ is a full transmitted wave and because λ_+ consists of at least one "high" barrier—at any rate the present argument is only applicable for energies below the barrier top—an approximate solution for $\phi_-(x)$ is a wave that is fully reflected by a wall. So we can write for $x\ll0$

$$\boldsymbol{\Phi}(x)\approx\boldsymbol{\Phi}_{-\infty}(x):=\begin{pmatrix}c_-\\ c_+\end{pmatrix}e^{ikx}+\begin{pmatrix}0\\ -c_+\end{pmatrix}e^{-ikx}$$

and for $x\gg0$

$$\boldsymbol{\Phi}(x)\approx\boldsymbol{\Phi}_{\infty}(x):=\begin{pmatrix}c_-\\ 0\end{pmatrix}e^{ikx}.$$

In order to determine the amplitudes $c_\pm$ we have to compare with the asymptotic form of the scattering solution for left incidence,

$$\boldsymbol{\Psi}(x)\approx\boldsymbol{\Psi}_{-\infty}(x):=\begin{pmatrix}1\\ 0\end{pmatrix}e^{ikx}+\begin{pmatrix}R_{11}^l\\ R_{21}^l\end{pmatrix}e^{-ikx}$$

if $x\ll0$ and

$$\boldsymbol{\Psi}(x)\approx\boldsymbol{\Psi}_{\infty}(x):=e^{ikx}\begin{pmatrix}T_{11}^l\\ T_{21}^l\end{pmatrix}$$

if $x\gg0$.

The transmission and reflection coefficients can now be approximately calculated for each case from the boundary conditions $\boldsymbol{\Phi}_{-\infty}(x)=\boldsymbol{U}(-\infty)\boldsymbol{\Psi}_{-\infty}(x)$ and $\boldsymbol{\Phi}_{\infty}(x)=\boldsymbol{U}(\infty)\boldsymbol{\Psi}_{\infty}(x)$.

The incidence from the right can be treated in a similar way. All the amplitudes are given in Table I, from which we can find, taking the squares, the transmission and reflection probabilities. We find a perfect diodic behavior only in case 12. The pumping potential and a reflecting potential $\hat{W}_1>0$ on its right and $W_2=0$ (case 1) is not enough to make a perfect diode. While there is still full reflection if the atom comes from the right, the transmission probability is only 1/2 when the atom comes from the left; accordingly there is a 1/2 reflection probability from the left, which is equally distributed between the ground- and excited-state channels.

The adiabatic picture provides in summary a simple explanation of the behavior of the diode and its variants. In particular, the perfect diode behavior of case 12, occurs because the (approximately) freely moving mode ϕ_- transfers adiabatically the ground state to the excited state from left to right. To visualize this, let us represent the probabilities to find the ground and excited state in the eigenvectors $|\lambda_-^{(j)}(x)\rangle$ for the cases $j=12,1$. They are plotted in Fig. 7(a) for the case 12: the perfect adiabatic transfer can be seen clearly. On the other hand, the mode + (not plotted), which tends to the ground state on the right edge of the device, is blocked by a high barrier. The stability of this blocking effect with respect to incident velocities holds for energies smaller than the λ_+ barrier top (more on this below). In Fig. 7(b) the ground and excited state probabilities for case 1 are plotted. If the mirror potential laser W_2 is removed on the left edge of the device, the ground state is not any more an eigenstate of the potential for $x\ll0$. The adiabatic transfer of the mode − occurs instead from $(|2\rangle-|1\rangle)/2^{1/2}$ on the left to $|2\rangle$ on the

TABLE I. Reflection and transmission probability for the different variations of the atom diode.

Case	$c_-^{r/l}$	$c_+^{r/l}$	$R_{11}^{r/l}$	$R_{21}^{r/l}$	$T_{11}^{r/l}$	$T_{21}^{r/l}$
(a) Incidence from the right						
(0) $\hat{W}_1=\hat{W}_2=0$	$-\frac{1}{\sqrt{2}}$	$\frac{1}{\sqrt{2}}$	$-\frac{1}{2}$	$-\frac{1}{2}$	$\frac{1}{2}$	$-\frac{1}{2}$
(1) $\hat{W}_1>0,\hat{W}_2=0$	0	1	−1	0	0	0
(2) $\hat{W}_1=0,\hat{W}_2>0$	$-\frac{1}{\sqrt{2}}$	$\frac{1}{\sqrt{2}}$	$-\frac{1}{2}$	$-\frac{1}{2}$	$\frac{1}{\sqrt{2}}$	0
(12) $\hat{W}_1>0,\hat{W}_2>0$	0	1	−1	0	0	0
(b) Incidence from the left						
(0) $\hat{W}_1=\hat{W}_2=0$	$-\frac{1}{\sqrt{2}}$	$\frac{1}{\sqrt{2}}$	$-\frac{1}{2}$	$-\frac{1}{2}$	$\frac{1}{2}$	$-\frac{1}{2}$
(1) $\hat{W}_1>0,\hat{W}_2=0$	$-\frac{1}{\sqrt{2}}$	$\frac{1}{\sqrt{2}}$	$-\frac{1}{2}$	$-\frac{1}{2}$	0	$-\frac{1}{\sqrt{2}}$
(2) $\hat{W}_1=0,\hat{W}_2>0$	−1	0	0	0	$\frac{1}{\sqrt{2}}$	$-\frac{1}{\sqrt{2}}$
(12) $\hat{W}_1>0,\hat{W}_2>0$	−1	0	0	0	0	−1

right, whereas the blocked mode + on the left corresponds to the linear combination $(|2\rangle+|1\rangle)/2^{1/2}$. This results in a 1/2 reflection probability for ground-state incidence from the left. A similar analysis would be applicable in the other cases.

The probabilities of Table I for the case 12 coincide with the results shown in Fig. 2. We also have calculated numerically the transmission and reflection probabilities for cases 1 and 2 shown in Fig. 8. The results also coincide with Table I and show again that the counterintuitive state-selective mirror W_2 is really important to attain a perfect diode.

Note that in the case 2 ($\hat{W}_1=0$, $\hat{W}_2>0$) there is no full reflection for incidence from the right in the ground state so this case is not useful as a diode. But for incidence from the left there is equal transmission in ground and excited states so that this device might be useful to build an interferometer.

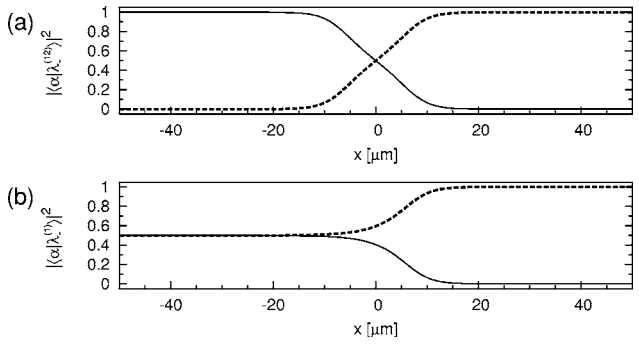

FIG. 7. $|\langle 1|\lambda_-^{(j)}\rangle|^2$ (solid lines) and $|\langle 2|\lambda_-^{(j)}\rangle|^2$ (dashed lines) for $d=50$ μm, $\hat{\Omega}=1\times10^6$/s, $\hat{W}_1=100\times10^6$/s; (a) $\hat{W}_2=100\times10^6$/s (case $j=12$), (b) $\hat{W}_2=0$ (case $j=1$).

B. Limits of the approximation

The approximations made so far have a range of validity that depends on the potential parameters and determines the working conditions of the diode. Even though these conditions can be easily found numerically from the exact results, approximate breakdown criteria are helpful to understand the limits of the device and different reasons for its failure.

For the approximation that ϕ_- is a fully transmitted wave and ϕ_+ a fully reflected one a necessary condition is

$$\max_x[\lambda_-(x)] < E_v < \max_x[\lambda_+(x)]. \tag{12}$$

This defines the limits

$$v_{\lambda,\min} := \sqrt{\frac{2}{m}\max_x[\lambda_-(x)]}, \tag{13}$$

$$v_{\lambda,\max} := \sqrt{\frac{2}{m}\max_x[\lambda_+(x)]}, \tag{14}$$

such that Eq. (12) is fulfilled for all v with $v_{\lambda,min}<v<v_{\lambda,max}$. The plateaus of v_{max} seen, e.g., in Fig. 3 for a range of d values are essentially coincident with $v_{\lambda,max}$.

Figure 9 shows an example of the case 0 (only a pumping laser, $\hat{W}_1=\hat{W}_2=0$). We see that the transmission and reflec-

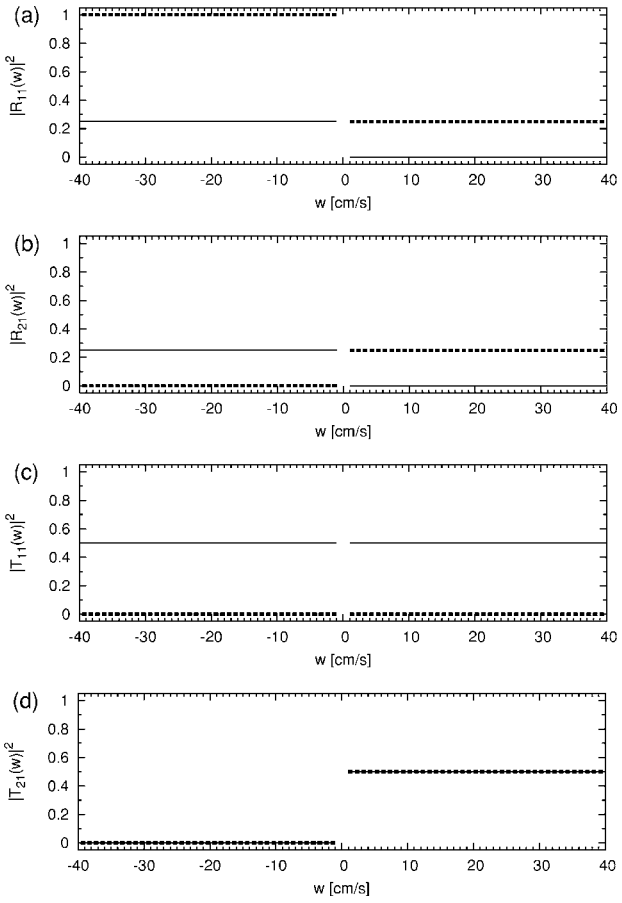

FIG. 8. (a) Reflection probability $|R_{11}(w)|^2$, (b) reflection probability $|R_{21}(w)|^2$, (c) transmission probability $|T_{11}(w)|^2$; (d) transmission probability $|T_{21}(w)|^2$; $d=50$ μm, $\hat{\Omega}=1\times10^6$/s; $\hat{W}_1=100\times10^6$/s, $\hat{W}_2=0$ (dashed lines); $\hat{W}_1=0$, $\hat{W}_2=100\times10^6$/s (solid lines).

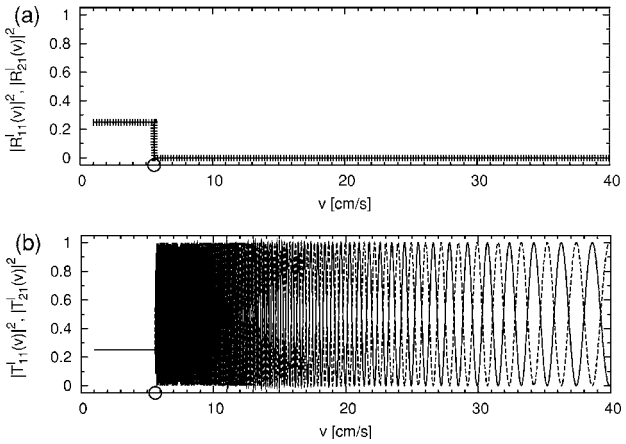

FIG. 9. Reflection and transmission probability for incidence from the left, $d=50$ μm, $\hat{\Omega}=1\times10^6$/s, $\hat{W}_1=\hat{W}_2=0$; the circles indicate $v_{\lambda,max}$ while in this case $v_{\lambda,min}=0$ [see Eqs. (13) and (14)]; (a) $|R^l_{11}(v)|^2$ (thick dotted line), $|R^l_{21}(v)|^2$ (solid line); (b) $|T^l_{11}(v)|^2$ (dashed line), $|T^l_{21}(v)|^2$ (solid line).

$$q(v) := \max_{x\in I} \frac{|A(x)|^2 + 2m|B(x)|^2[E_v - \lambda_-(x)]}{|\lambda_+(x) - \lambda_-(x)|^2} \ll 1 \tag{15}$$

with $I=[-d,d]$. A velocity boundary $v_{ad,max}$ defined by $q(v)<\epsilon$ for all $v_{\lambda,min}<v<v_{ad,max}$ is shown in Fig. 10 with $\epsilon=0.01$. [Note that the condition of Eq. (15) only makes sense if $E_v>\lambda_-(x)$, i.e., $v_{\lambda,min}<v$.] We see in Fig. 10 that we have the same qualitative dependence of v_{max} on d and of $v_{ad,max}$ on d. Therefore the breakdown of the diode at v_{max} for large d is due to a failure of the adiabatic approximation.

The same ideas are applicable to the dependence on the pulse shape (see Fig. 5). The decrease of the upper limit for larger a is also due to a failure of the adiabatic approximation.

tion probabilities are approximately velocity independent and all channels are equally populated until $v_{\lambda,max}$ (in coincidence with Table I). From this point on, Rabi oscillations start (for a related effect see [14]). Note that, if mirror potentials are added to the pumping laser (as in Fig. 8), this implies a noteworthy stabilization of the probabilities and velocity independence in comparison to Fig. 9.

Figure 10 shows the exact limits v_{min} and v_{max} for the diodic behavior for different d (see also Fig. 3) for the perfect diode case 12. The limits $v_{\lambda,min}$, $v_{\lambda,max}$ resulting from the condition of Eq. (12) are also shown. We see that the exact limit v_{min} coincides essentially with $v_{\lambda,min}$ so that the lower diodic velocity boundary can be understood by the breakdown of the condition that ϕ_- is fully transmitted due to a λ_- barrier. This effect is only relevant for small distances d between the lasers.

Another reason for the breaking down of the diode may be that the adiabatic modes are no longer independent, i.e., that $\boldsymbol{Q}$ [see Eq. (9)] cannot be neglected. An approximate criterion for adiabaticity, more precisely for neglecting the nondiagonal elements of $\boldsymbol{Q}$ (see the Appendix) is

V. SUMMARY

Summarizing, we have examined a two-level model for an atom diode, a laser device in which ground-state atoms can pass in one direction but not in the opposite direction. The proposed scheme includes two state-selective mirrors, one for the excited state on the left, the other one for the

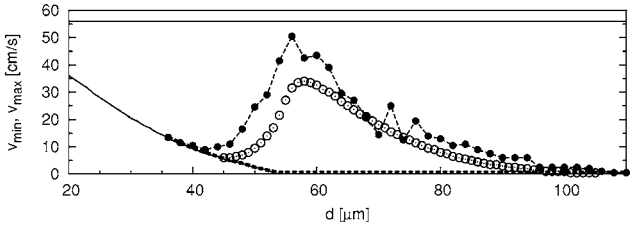

FIG. 10. Limits of the diodic behavior v_{min} (thick dashed line) and v_{max} (filled circles connected with a dashed line); limits of condition (12) $v_{\lambda,min}$ (lower solid line) and $v_{\lambda,max}$ (upper solid line); limit of the adiabatic approximation $v_{ad,max}$ (unfilled circles); $\hat{W}_1=\hat{W}_2=100\times10^6$/s, $\hat{\Omega}=0.2\times10^6$/s.

ground state on the right, and a pumping region—located between the two mirrors—on resonance with the atomic transition. Note that this scheme can be realized by a highly detuned three-level STIRAP transfer.

We have shown that the diodic behavior is very stable with respect to atom velocity in a given range, and with respect to changes in the distances between the centers of the lasers and the pulse shapes. The inclusion of the laser on the left, reflecting the excited state, is somewhat counterintuitive, but it is essential for a perfect diode effect; the absence of this laser leads to a 50% drop in efficiency.

The stability properties as well as the actual mechanism of the diode are explained with an adiabatic basis and an adiabatic approximation. The diodic transmission is due to the adiabatic transfer of population from left to right, from the ground state to the excited state in a free-motion adiabatic mode, while the other mode is blocked by a barrier.

ACKNOWLEDGMENTS

We thank V. Hannstein for comments. J.G.M. is grateful to D. Guéry-Odelin and C. Salomon for a fruitful visit to the Kastler Brossel Laboratory (Paris). A.R. acknowledges support by the Ministerio de Educación y Ciencia and the German Academic Exchange Service (DAAD). This work has been supported by Ministerio de Educación y Ciencia (Grant No. BFM2003-01003), and UPV-EHU (Grant No. 00039.310-15968/2004).

APPENDIX

To motivate Eq. (15) (see also [15]) let us assume

$$E\mathbf{\Phi}(x) = -\frac{\hbar^2}{2m}\frac{\partial^2}{\partial x^2}\mathbf{\Phi}(x) + \begin{pmatrix} \lambda_- & 0 \\ 0 & \lambda_+ \end{pmatrix}\mathbf{\Phi}(x) + \epsilon\begin{pmatrix} 0 & -\tilde{A} + i\tilde{B}\hat{p}_x \\ \tilde{A} - i\tilde{B}\hat{p}_x & 0 \end{pmatrix}\mathbf{\Phi}(x) \qquad \text{(A1)}$$

where $\lambda_\pm$, $\tilde{A}$, and $\tilde{B}$ are real and independent of x. We assume that $E > \lambda_-$ and that ϵ is small such that we can treat $\mathbf{\Phi}$ perturbatively,

$$\mathbf{\Phi}(x) \approx \begin{pmatrix} \phi_{0,-}(x) \\ \phi_{0,+}(x) \end{pmatrix} + \epsilon\begin{pmatrix} \phi_{1,-}(x) \\ \phi_{1,+}(x) \end{pmatrix}$$

with

$$\phi_{0,-}(x) = \exp\left(\frac{i}{\hbar}\sqrt{2m(E-\lambda_-)}x\right),$$

$$\phi_{0,+}(x) = 0.$$

Then it follows from Eq. (A1) for the first-order correction

$$\phi_{1,-} = 0,$$

$$\phi_{1,+} = [E - \lambda_+ - \hat{p}_x^2/(2m)]^{-1}(\tilde{A} - i\tilde{B}\hat{p}_x)\phi_{0,-} = \frac{\tilde{A} - i\tilde{B}\sqrt{2m(E-\lambda_-)}}{\lambda_- - \lambda_+}\phi_{0,-}$$

because $\hat{p}_x\phi_{0,-} = \sqrt{2m(E-\lambda_-)}\phi_{0,-}$. If we want to neglect $\phi_+ = 0 + \epsilon\phi_{1,+}$ we get the condition

$$\epsilon^2\frac{|\tilde{A}|^2 + |\tilde{B}|^2 2m(E-\lambda_-)}{|\lambda_- - \lambda_+|^2} \ll 1.$$

If $\lambda_\pm$, $\tilde{A}$ and $\tilde{B}$ depend on x, we may use the condition

$$\max_{x\in I}\frac{|\epsilon\tilde{A}(x)|^2 + |\epsilon\tilde{B}(x)|^2 2m[E-\lambda_-(x)]}{|\lambda_-(x) - \lambda_+(x)|^2} \ll 1$$

where I is chosen in such a way that the assumption $\phi_{0,+}(x) = 0$ is approximately valid.

In Eq. (A1), we have not included any diagonal elements in the coupling, compare with Eq. (9). We neglect them in the condition (15) but in principle it would be also possible to absorb them by defining effective adiabatic potentials $\tilde{\lambda}_\pm = \lambda_\pm + mB^2/2$.

[1] A. Ruschhaupt and J. G. Muga, Phys. Rev. A **70**, 061604(R) (2004).
[2] M. G. Raizen, A. M. Dudarev, Qian Niu, and N. J. Fisch, Phys. Rev. Lett. **94**, 053003 (2005).
[3] A. M. Dudarev, M. Marder, Qian Niu, N. J. Fisch, and M. G. Raizen, Europhys. Lett. **70**, 761 (2005).
[4] K. Bergmann, H. Theuer, and B. W. Shore, Rev. Mod. Phys. **70**, 1003 (1998).
[5] D. Schneble, M. Hasuo, T. Anker, T. Pfau, and J. Mlynek, J. Opt. Soc. Am. B **20**, 648 (2003).
[6] R. Folman, P. Krüger, J. Schmiedmayer, J. Denschlag, and C. Henkel, Adv. At., Mol., Opt. Phys. **48**, 263 (2002).
[7] V. Hannstein, G. C. Hegerfeldt, and J. G. Muga, J. Phys. B **38**, 409 (2005).
[8] A. Ruschhaupt, J. A. Damborenea, B. Navarro, J. G. Muga, and G. C. Hegerfeldt, Europhys. Lett. **67**, 1 (2004).
[9] C. Cohen-Tannoudji, in *Fundamental Systems in Quantum Optics*, edited by J. Dalibard, J.-M. Raimond, and J. Zinn-Justin (North-Holland, Amsterdam, 1992), p. 3.
[10] S. Singer, K. F. Freed, and Y. B. Band, J. Chem. Phys. **77**, 1942 (1982).
[11] Y. B. Band and I. Tuvi, J. Chem. Phys. **100**, 8869 (1994).
[12] H. Shen, J.-P. Dussault, and A. D. Bandrauk, Chem. Phys. Lett. **221**, 498 (1994).
[13] V. S. Malinovsky and D. J. Tannor, Phys. Rev. A **56**, 4929 (1997).
[14] B. Navarro, I. L. Egusquiza, J. G. Muga, and G. C. Hegerfeldt, Phys. Rev. A **67**, 063819 (2003).
[15] A. Messiah, *Quantum Mechanics* (Wiley, New York, 1958).